

CLO: Efficient LLM Inference System with CPU-Light KVCache Offloading via Algorithm-System Co-Design

Jiawei Yi

jiaweiyi@mail.ustc.edu.cn

University of Science and Technology
of China
Hefei, Anhui, China

Jiaqi Ruan

jiaqiruan@mail.ustc.edu.cn

University of Science and Technology
of China
Hefei, Anhui, China

Haibo Wang

wanghaibo33@huawei.com

Huawei Technologies Co., Ltd
China

Feng Wu

fengwu@ustc.edu.cn

University of Science and Technology
of China
Hefei, Anhui, China

Ping Gong

gpzlx1@mail.ustc.edu.cn

University of Science and Technology
of China
Hefei, Anhui, China

Shengnan Wang

wsn511799@163.com

Independent Researcher
China

Weiguang Wang

weiguang.wang@huawei.com

Huawei Technologies Co., Ltd
China

Youhui Bai

youhuibai@ustc.edu.cn

University of Science and Technology
of China
Hefei, Anhui, China

Pengcheng Wang

wangpengcheng25@huawei.com

Huawei Technologies Co., Ltd
China

Xia Zhu

zhuxia1@huawei.com

Huawei Technologies Co., Ltd
China

Cheng Li

chengli7@ustc.edu.cn

University of Science and Technology
of China
Hefei, Anhui, China

Abstract

The growth of million-token LLMs exposes the scalability limits of inference systems, where the KVCache dominates memory usage and data transfer overhead. Recent offloading systems migrate the KVCache to CPU memory and incorporate top- k attention to reduce the volume of data transferred from the CPU, while further applying system-level optimizations such as on-GPU caching and prefetching to lower transfer overhead. However, they overlook the CPU bottleneck in three aspects: (1) substantial overhead of fine-grained dynamic cache management performed on the CPU side, (2) significant transfer overhead from poor PCIe bandwidth utilization caused by heavy gathering operations at the CPU side, and (3) GPU runtime bubbles introduced by coarse-grained CPU-centric synchronization.

To address these challenges, we propose CLO, a CPU-light KVCache offloading system via algorithm-system co-design. CLO features: (1) a coarse-grained head-wise approximate on-GPU caching strategy with negligible cache management cost, (2) seamless combination of data prefetching and on-GPU persistent caching for lower transfer overhead, (3) a zero-copy transfer engine to fully exploit PCIe bandwidth, and a GPU-centric synchronization method to eliminate GPU stalls. Evaluation on two widely-used LLMs demonstrates that CLO achieves comparable accuracy to state-of-the-art systems, while substantially minimizing CPU overhead, fully utilizing PCIe bandwidth, thus improving

decoding throughput by 9.3%-66.6%. Our results highlight that algorithm-system co-design is essential for memory-constrained LLM inference on modern GPU platforms. We open source CLO at <https://github.com/CommediaJW/CLO>.

1 Introduction

In recent years, generative large language models (LLMs) [41] have been widely adopted in real-world applications, such as natural language processing [30], code generation [14], and multimodal tasks [49]. During the autoregressive inference of LLMs, the key-value pairs of historical tokens (well-known as KVCache) are stored in GPU memory for generating subsequent tokens, avoiding redundant computation. However, both the KVCache storage and KVCache loading grow linearly with sequence length and batch size (i.e. the number of requests). With the rising popularity of long-context tasks such as document summarization [15] and multi-turn dialogue [8], the sequence length supported by modern LLMs has expanded dramatically, reaching up to 1 million tokens, as exemplified by models like Llama3 [27] and Qwen2.5 [32]. In addition, existing inference systems typically employ large batch sizes to increase system throughput and improve resource utilization. These make the data loading overhead from the KVCache, along with its memory footprint, primary bottlenecks that restrict the performance of inference systems.

To address loading overhead from the full GPU cache, recent works leveraged the inherent sparsity of attention mechanism [10, 33] and proposed top- k attention algorithms [9, 33, 38, 40]. These algorithms only fetch a small critical subset of the KVCache for computation, thereby reducing the data loading volume and improving the inference throughput. However, top- k attention fails to resolve the KVCache memory consumption problem. For instance, in Qwen2.5-14B-Instruct-1M [32] model, the KVCache memory reaches 93.75 GB for a 512K sequence length, far exceeding the typical capacity of a single modern GPU [23–25].

To resolve this issue, state-of-the-art systems [5, 16, 45, 50] offload the full KVCache to host memory and integrate top- k attention to reduce the PCIe transfer volume. For further reduction of the transfer overhead, two system-level optimizations are proposed, *GPU caching* and *prefetching*. The *GPU caching* caches frequently accessed top- k KV data in spare GPU memory and manages it with fine-grained cache management policies such as LRU [26] or LFU [34], thereby reducing the overhead of loading data from the CPU memory. The *prefetching* leverages the similarity of hidden states across adjacent LLM layers to predict the top- k KV of the next layer in advance, enabling its loading process to overlap with the computation of the current layer.

Despite the optimizations, these systems still suffer from a remarkable performance gap compared with the full on-GPU KVCache. First, for GPU caching, fine-grained block-wise dynamic caching strategies can significantly improve hit ratios, but the list-based data structures used for cache management fail to exploit the inherent parallelism of GPUs and must be handled by the CPU, leaving prohibitive management costs. This overhead is most evident in *cache updates*, where *top- k KV / block_size* entries must be modified one by one for each attention head per inference step. Moreover, aggressively pursuing high cache hit rates may leave PCIe resources idle and wasted. Second, at the opposite extreme, the prefetching does not employ on-GPU caching but transfers all top- k KV data over low-bandwidth PCIe, where a CPU-side gathering with significant overhead is required beforehand, leading to underutilization of PCIe bandwidth and dramatic transfer overhead. A similar CPU-side bottleneck is observed in the cache miss handling of GPU caching approaches. Finally, traditional CPU-centric CPU-GPU synchronization additionally incurs a constant overhead per synchronization event, which is independent of the transferred data size and scales only with the frequency of synchronization. Through the above analysis, we observe that the CPU, often overlooked in prior works, plays a critical role in the trade-offs of cache hit rate, management overhead, and data transfer costs.

Motivated by these observations, we propose CLO, a CPU-Light KVCache Offloading inference system via algorithm and system co-design. It aims to address the CPU bottlenecks overlooked by existing systems, fully exploiting the potential performance gains from GPU caching and saturated PCIe

bandwidth. At a high level, we strike a balance between the overhead of cache management and data transfer caused by cache misses. On the one hand, instead of using highly accurate cache algorithms, we propose an approximate caching strategy, trading cache hits for eliminating the cache management overhead at the CPU side. On the other hand, to compensate for cache miss overhead, we try to optimize the loading path systematically. Ultimately, both parts can be seamlessly integrated, simultaneously reducing cache management overhead while fully hiding data transfer costs.

Specifically, CLO makes three key technical contributions. First, to ease GPU cache management, we make two key observations. KV vectors can be largely reused across queries of a few adjacent inference steps, which are easy to capture, but not affordable by advanced cache algorithms. Furthermore, we rethink the granularity from head or KV block and choose head, maintain only a single metadata entry per attention head, and perform at most one cache update per inference step (no update when cache hit), thereby incurring lower overhead. Combining these two, our new cache algorithm renders negligible management overhead and opens opportunities for further system optimizations.

Second, we observe that KV vectors corresponding to cache misses can be further divided into two types. Inference accuracy-critical vectors are kept resident in GPU memory to guarantee immediate availability, while accuracy-trivial ones are prefetched based on query similarity across adjacent layers. This selective residency combined with similarity-driven prefetching ensures that the miss data is served directly from GPU memory or the loading overhead is hidden by computation, resulting in minimal overhead to inference throughput.

Finally, we develop a zero-copy transfer engine to fully utilize the PCIe bandwidth and redesign a GPU-centric synchronization mechanism to eliminate the kernel launch overhead, further alleviating the CPU pressure.

We conduct extensive experiments using two widely-used LLM models on a GPU with 48 GB memory. Compared with state-of-the-art KVCache offloading systems, CLO achieves comparable inference accuracy while improving inference throughput by 9.3%–66.6%. Further analysis shows that CLO incurs negligible cache management overhead, improves PCIe bandwidth utilization to theoretical peak, and completely eliminates kernel launch overhead.

2 Background and Motivation

2.1 LLM Inference and Top- k Attention

In large language models (LLMs), the attention module plays a role in capturing the semantic relationships between input tokens, which is crucial for language modeling. Generally, the attention module includes h individual heads, which is also called *multi-head attention* (MHA)[41]. Given the input hidden states $\mathbf{X} \in \mathbb{R}^{n \times d}$ (n indicates sequence length and d is the hidden dimension), each attention head i first projects \mathbf{X}

via head-specific weight matrices $\mathbf{W}_Q^i, \mathbf{W}_K^i, \mathbf{W}_V^i \in \mathbb{R}^{d \times d_k}$ into Query, Key, and Value vectors ($\mathbf{Q}_i, \mathbf{K}_i, \mathbf{V}_i \in \mathbb{R}^{n \times d_k}$), where $d_k = d/h$, and then computes $\mathbf{O}_i = \text{softmax} \left(\mathbf{Q}_i \mathbf{K}_i^\top / \sqrt{d_k} \right) \mathbf{V}_i$. The outputs of all the heads are concatenated as $\text{Concat}(\mathbf{O}_0, \dots, \mathbf{O}_{h-1}) \in \mathbb{R}^{n \times d}$ and projected via $\mathbf{W}_O \in \mathbb{R}^{d \times d}$ to produce the final output. In addition, modern LLMs [20, 27, 32] further employ the *Grouped-Query Attention* (GQA) mechanism, which reduces the number of KV heads by grouping multiple query heads to share a single KV head.

Generally, LLM inference generates tokens autoregressively, and it can be divided into two distinct phases, *prefill* and *decoding*. The prefill phase processes the full prompt in parallel to generate the first token, and meanwhile caches the KV vectors in GPU HBM, which is called KVCache. After this, the decoding phase produces tokens sequentially based on the KVCache and updates it step-by-step. The KVCache scales linearly with the number of tokens, so its size inflates drastically as the input sequence length and batch size increases. Note that tasks such as multi-turn conversation [8], document summarization [15], and code understanding [4] often involve extremely long contexts, and on the other hand, modern inference platforms prefer large batch size for higher throughput. Consequently, KVCache storage and loading emerge as critical performance bottlenecks in LLM inference [33]. For example, on Qwen2.5-14B-Instruct-1M [32], a 512K sequence requires 93.75 GB of KVCache, 3.3 \times its 28 GB model weights.

To accelerate KVCache loading, top- k attention has been proposed. It exploits the inherent sparsity of attention [10, 33], achieving near-lossless inference accuracy by loading only a small but critical subset of KVCache for computation. Advanced top- k attention algorithms such as Quest [40], HATA [9], and Loki [38] focus on efficiently identifying the critical KV pairs. To this end, they generate compact *retrieval metadata* derived from the KCache, such as token block descriptors [40], hash codes [9], and critical channels [38], to facilitate top- k KV selection. This process can be uniformly formalized as:

$$\text{Metadata} = \text{Encode}(K\text{Cache}) \quad (1)$$

$$\text{Index} = \text{Retrieval}(q, \text{Metadata}) \quad (2)$$

$$K_{TopK}, V_{TopK} = \text{Gather}(K\text{Cache}, V\text{Cache}, \text{Index}) \quad (3)$$

$$o_{TopKattn} = \text{softmax} \left(q K_{TopK}^\top / \sqrt{d_k} \right) V_{TopK} \quad (4)$$

The metadata is typically one or several orders of magnitude smaller than the original KVCache. For instance, under default configurations of Quest [40], Loki [38], and HATA [9], metadata consumes only 12.5%, 12.5%, and 3.1% of the total KVCache size, respectively.

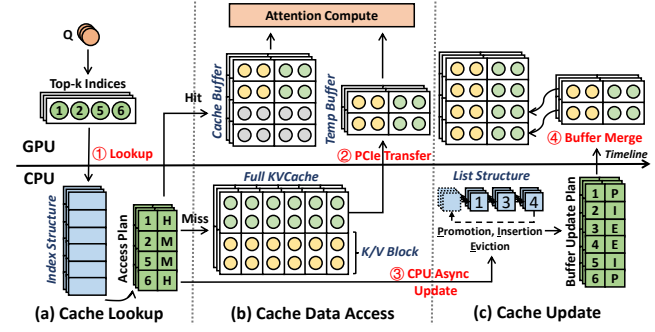


Figure 1. Overview of RetroInfer [5]’s caching policy. PQCache [50] follows a similar workflow but performs cache lookup on GPU.

2.2 KVCache Optimizations

Though the KVCache loading issue is alleviated, due to the growing KVCache size and heavy GPU HBM usage, KVCache storage is still a critical challenge. Existing systems [5, 16, 36, 45, 50] choose to offload the KVCache to host memory to mitigate the HBM memory consumption. In addition, they integrate top- k attention to reduce the KV data volume transferred from CPU to GPU. For fast lookup, generally the compact retrieval metadata is retained in GPU HBM so that the PCIe bandwidth can be reserved exclusively for KV data transfer. Though the transmission of KV data is greatly reduced, it is still a performance bottleneck, due to limited bandwidth of PCIe. To further enhance efficiency, two categories of system-level optimizations have been explored.

2.2.1 Prefetching. This technique tried to overlap the PCIe transfer with inference computation on GPU through prefetching the top- k KV data, introduced by InfiniGen [16]. Leveraging the high similarity between hidden states of adjacent LLM layers, InfiniGen is able to predict the important KV data to be transferred of next layer in advance, hence earning the opportunities for compute-loading overlap. Specifically, at the beginning of layer $l-1$, it approximates the query vector of layer l ’s by

$$q_{approx}^l = x^{l-1} W_Q^l, \quad (5)$$

using which the approximate top- k selection of layer l can be obtained one layer ahead and the KV transmission of layer l can then be overlapped with the computation of layer $l-1$. This strategy is known as *speculative sparse prefetching*.

2.2.2 GPU Caching. Most recently, PQCache [50] and RetroInfer [5] have introduced dynamic GPU caches with fine-grained, list-based policies like LRU [26] and LFU [34] to reduce PCIe data transfer. These systems exploit the GPU HBM freed by offloading the KVCache to host memory to cache frequently accessed top- k KV data. To simplify the management and transfer of cache data, they bundle consecutive key-value vectors into *blocks*, typically ranging from

Table 1. Summary of cache management strategies of RetroInfer [5], PQCache [50] and CLO.

System	Granularity	Cache Lookup			Cache Metadata Update			Cache Buffer Update	
		Data Structure	Manager	Overhead	Data Structure	Manager	Overhead	Extra Copy	Overhead
RetroInfer	KV Block	Index Map	CPU	Middle	LRU Linked List	CPU	High	Y	High
PQCache	KV Block	Index Map	GPU	Low	LFU Linked List	CPU	High	Y	High
CLO (ours)	KV Head	Query Vectors	GPU	Negligible	Query Vectors	GPU	Negligible	N	None

tens to hundreds of tokens. For a single sequence, each attention head within a LLM layer maintains independent cache metadata and buffers.

As illustrated in Figure 1, the GPU caching workflow for decoding phase involves three stages. First, during *cache lookup*, GPU generates top- k indices which the CPU uses to lookup an *index structure* (e.g., hash map) and constructs an access plan annotated with cache hit/miss information. Second, in *cache data access*, according to the access plan, hit data is directly served from the HBM cache buffer while misses are fetched via PCIe from the CPU’s full KVCache into a GPU temporary buffer, after which attention computation occurs. Third, during *cache update*, CPU updates *all the accessed blocks’ metadata* within *list structure*, performing promotion, eviction, insertion, while generating an update plan for GPU to merge missed data into the cache buffer.

List structure is the core component, typically organized as a linked list. Each of its entry corresponds to a block’s metadata, such as its index in cache buffer, and block states maintained for cache replacement, like recency for LRU [26] / ARC [19], and frequency for LFU [34] / LeCaR [42].

According to [31, 35], list-based caches exhibit low concurrency and demand strong consistency, making them better suited for CPU management. However, CPU-based management lags behind GPU computation. To hide its overhead, SOTA systems overlap list updates with PCIe transfers and attention computation. However, this approach leads to extra data copying within GPU HBM, i.e., the buffer merge depicted in Figure 1. Worse still, even with asynchronous execution, the update overhead may not be completely overlapped. We summarize the cache management strategies of existing works in Table 1, all of which suffer from significant overhead due to metadata updates and buffer merging.

2.3 Limitations of Existing Works

Despite the above optimizations, a performance gap remains compared with the ideal case with a sufficient large GPU HBM to store the full KVCache. As Figure 2 shows, the per-layer decoding latency of RetroInfer, InfiniGen, and PQCache rises to 137%, 337%, and 354% against the ideal, mainly due to three factors:

Cache management involves the cache lookup and update operations detailed in Section 2.2, particularly the CPU-based linked list maintenance.

Host data transfer involves transferring the required top- k KV data to GPU HBM via PCIe, the latency is determined

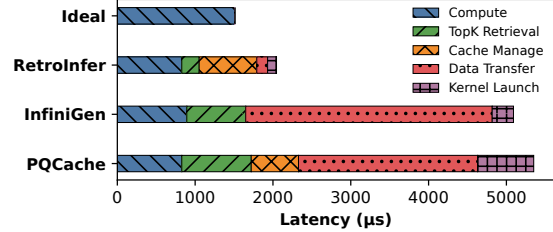


Figure 2. Per-layer decoding latency breakdown of existing works and the ideal case (full KVCache resides in GPU HBM). Sequence length=128K, batch size=1 and top- k ratio=10%. Evaluated on Llama3-8B-1048K model [27].

Table 2. Cache hit ratios of RetroInfer [5] and PQCache [50] (top- k ratio=10%, batch size=1), evaluated on RULER’s VT benchmark [11] using Llama3-8B-1048K [27]. Cache capacity = 3×top- k KV size (30% of the whole KVCache).

SeqLen	4K	8K	16K	32k	64k	128k
RetroInfer	95%	94%	93%	92%	93%	93%
PQCache	39%	40%	37%	37%	37%	36%

by both the data volume and the PCIe bandwidth utilization. For InfiniGen, this overhead refers to the unoverlapped part. **Control and synchronization** are required to ensure data readiness of CPU-GPU coordination, including the transfer of KV data and cache metadata (e.g., indices for cache lookup). However, traditional synchronization approaches (e.g. cudaStreamSynchronize) are CPU-centric, which block CPU from launching subsequent GPU kernels. The CPU can only launch these kernels after the synchronization completes, introducing bubbles of tens to hundreds of microseconds into the GPU computation stream. This overhead is primarily determined by synchronization frequency, independent of the data volume being transferred.

Next, we zoom in Figure 2. Among these systems, RetroInfer demonstrates the lowest data transfer overhead due to 90% cache hit rate (Table 2), but suffers remarkable cache management overhead, up to 36.2% of total latency (its high hit ratio also implies underutilized PCIe resources). At the opposite extreme, InfiniGen relies solely on prefetching to reduce transfer overhead, while the substantial data volumes prevent transmission from being fully overlapped, resulting in 62.2% non-overlapped overhead. PQCache represents a hybrid approach with lower hit ratio (40%), yielding 43.0% transfer overhead falling between RetroInfer and InfiniGen.

Although the cache management accounts for only 11.3% of latency, the absolute cost is comparable to RetroInfer (607 μ s vs. 739 μ s) due to the linked list updates regardless of hit rate (Section 2.2). Consequently, the cumulative overhead across both dimensions renders PQCache the worst-performing among the three systems.

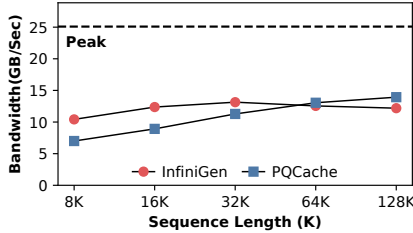


Figure 3. Achieved PCIe bandwidth of host data gathering and transfer process in **InfiniGen** and **PQCache**. Batch size=1 and top- k ratio=10%, evaluated on Llama3-8B-1048K model [27], with 64 CPU threads for data gathering.

In addition, our analysis reveals that the host data transfer overhead in InfiniGen and PQCache arises not only from large transfer volumes but also from their low PCIe bandwidth utilization. Figure 3 illustrates their achieved PCIe bandwidth under different transfer volumes, consistently below the peak. This is due to their non-zero-copy transfer mechanisms, which gather scattered KV data in host memory before PCIe transmission and thus incur high overhead.

Beyond data transfer and cache management overheads, synchronization-induced kernel launch overheads also affect decoding latency. RetroInfer incurs 5.5% overhead from synchronization caused by transferring cache management metadata between CPU and GPU. InfiniGen, with more small GPU kernels and primarily synchronizes KV data transfers, experiences higher overhead (273 μ s vs. 114 μ s of RetroInfer). PQCache suffers the most overhead (13.5%) due to frequent synchronizations for both KV data and cache metadata.

2.4 Trade-offs

Based on the aforementioned results, we observe significant trade-offs across multiple dimensions. On the one hand, existing systems all suffer from severe CPU bottlenecks, caused by cache management of fine-grained dynamic cache strategies, CPU gathering overhead during data transfer, and synchronization-induced kernel launching overhead. On the other hand, they fail to fully utilize the hardware resources. InfiniGen obtains the top- k KV data purely from host memory, resulting in large-volume data transferred through PCIe while leaving spare GPU memory. In contrast, RetroInfer aggressively pursues high hit ratio, but leaves the PCIe bandwidth idle. Moreover, systems attempting to simultaneously exploit both resources fail to achieve the desired effect due to CPU bottleneck, as observed in PQCache.

Based on the above analysis, it is imperative to first address the CPU bottlenecks, thereby fully exploiting the potential performance gains from GPU caching and saturated PCIe bandwidth. To achieve this, we propose redesigning a CPU-light caching algorithm that may sacrifice cache hit ratio but greatly reduce management overhead. For cache misses, we adopt system-level optimizations to fully utilize PCIe bandwidth, potentially combining prefetching to hide data movement overhead within GPU computation. Through these optimizations, we can minimize CPU overhead and maximize PCIe utilization to achieve inference performance comparable to or even better than that of full GPU KVCache.

Nonetheless, achieving these objectives poses key challenges: (1) the trade-offs depend on multiple factors, including model architectures, workloads, and hardware configurations, requiring intelligent decisions. (2) Integrating novel caching and optimization techniques may affect inference accuracy, necessitating robust methodologies to ensure computational precision.

3 Cache Design

Based on the analysis in Section 2, the existing top- k attention based offloading systems with GPU caching suffer from substantial cache update overhead. To tackle this issue, we propose an efficient head-wise approximate caching strategy, leveraging the cosine similarity between queries. The proposed method provides a low-cost cache metadata update and eliminates extra buffer copying, and meanwhile maintains a low cache lookup overhead.

3.1 Query Similarity-based Approximate Cache

We observe that query vectors from adjacent few steps exhibit high cosine similarity, as shown in Figure 4. Figure 5 further illustrates the average cosine similarities of adjacent query pairs from each attention head, demonstrating the generality of this characteristic. Note that given a query q and a key k , the $qkscore$ is measured by

$$\text{dot-product}(q, k) = q^T k = ||q|| * ||k|| \cos(q, k). \quad (6)$$

Though the $qkscore$ of a single qk pair is related to both the direction and the length of vector q , the relative ordering of $qkscores$ between q and all keys is independent of $||q||$ since $||q||$ is shared. Hence the high cosine similarity of the adjacent queries implies high probability of them hitting same KV vectors under the top- k attention mechanism. As shown in Figure 6, higher cosine similarity correlates with greater top- k overlap.

These key observations motivate us to propose a fast approximate caching mechanism. We now detail its management workflow.

Initialization. At the initial decoding step 0, for each attention head i , we cache the query and selected top- k KV vectors in GPU HBM, denoted by q_c^i, K_c^i, V_c^i , namely *query label* and *cache data buffer*.

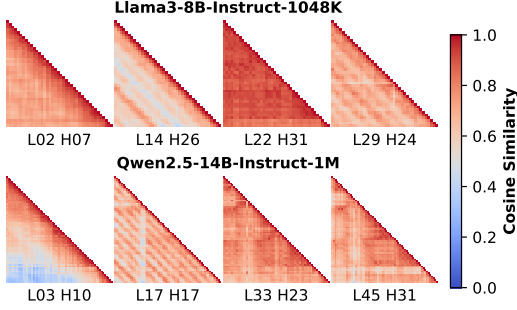


Figure 4. The cosine similarity distribution among query vectors. Evaluated on the decoding phase of a random sampled sequence. "L02 H07" means layer2 and head7. Adjacent queries (near the diagonal) exhibit high cosine similarity.

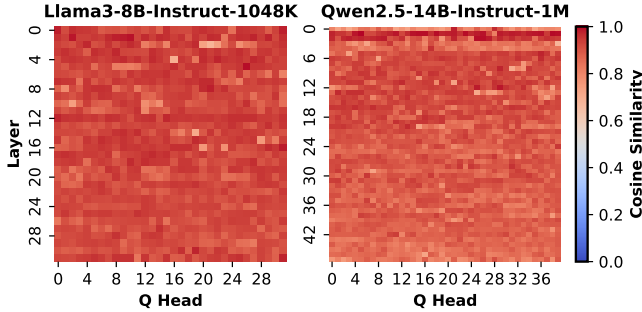


Figure 5. The average cosine similarity of queries from adjacent decoding steps. Evaluated on 30 random sampled sequences. High directional similarity is observed across models, layers and heads.

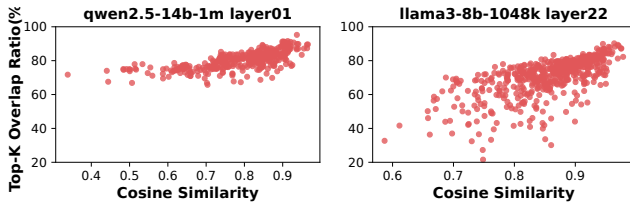


Figure 6. The relationship of adjacent query pair (q_0, q_1) 's cosine similarity and the overlap ratio of their top- k KV data. Evaluated on sequences randomly sampled from RULER-128K, measured at head granularity. Top- k ratio=10%.

Cache lookup. In an inference step $t > 0$, as shown in Figure 7, for each head i , if $\text{CosSim}(q_t^i, q_c^i) \geq \tau_i$ (a pre-defined threshold), this head is viewed as "cache hit" and q_t^i directly uses the cached K_c^i, V_c^i as its top- k KV vectors for computing top- k attention as shown in Equation (4). Otherwise, this head is marked as "cache miss", its q_t^i, K_c^i, V_c^i will be replaced in the cache update phase. This lookup operation only involves query similarity calculation, which can be accelerated through parallelism and GPU tensor cores, delivering a higher lookup efficiency, compared with existing systems.

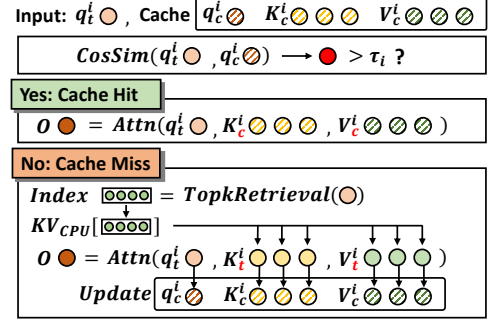


Figure 7. Workflow of query similarity-based approximate cache.

Cache update. For the missing heads of step t , both its query label and cache buffer data need to be updated. As shown in Figure 7, we reselect the actual top- k KV vectors, denoted by K_t^i, V_t^i , according to q_t^i . Query label q_t^i is updated to q_t^i , and the cached K_c^i, V_c^i will be replaced by K_t^i, V_t^i after they are fetched from the host memory. Compared to existing systems, this update process is remarkably simplified, delivering negligible overhead. First, it avoids the need for maintaining complex metadata structures (e.g., linked lists). Instead, it only needs to update a single query vector for one head, thereby significantly reducing the metadata update overhead. Second, the update plan of the cache data buffer only depends on the result of cache lookup. Thus, unlike existing systems, where the fetched host data are stored in a temporary HBM buffer and can be merged only after the slow metadata update process gives a buffer update plan (see Section 2.2 for details), our cache can write K_t^i, V_t^i directly to their final destinations, eliminating redundant data copying.

We summarize the differences between our cache strategy and those of existing systems in Table 1 to provide a clear comparative view.

Sink and recent tokens. According to [47], the sink tokens (the first several tokens of the sequence) and recent tokens are necessary to preserve accuracy. In this paper, we also adopt this trick and keep 4 sink tokens and 64 recent tokens, as suggested by [5, 46, 51]. We allocate a dedicated buffer in the cache to persistently store the KV vectors of these tokens, which avoids eviction during cache update.

3.2 Head Importance Awareness

3.2.1 Challenges. Despite its lightweight design, this cache strategy still faces the following challenges.

Accuracy-performance trade-off. The thresholds τ_i are important hyper-parameters that affect both accuracy and performance of the proposed approximate caching method. A lower value of τ_i implies high-frequency reuse of the cached data and low-frequency cache update, contributing to a high inference efficiency. However, in this situation, the query may miss actually important KV vectors, which leads to accuracy degradation. On the contrary, a higher value of τ_i may

achieve a high accuracy but a low efficiency. Therefore, how to configure the reuse thresholds to balance performance and accuracy emerges as the pivotal challenge.

Supporting GQA. To align with the widely-used GQA, data loading and caching must operate at KV-head granularity. However, cosine similarity computation occurs per query head. As a result, an effective intra-GQA similarity aggregation method is required to bridge the gap between KV heads and query heads.

3.2.2 Solutions. Duo-Attention [46] observed the unequal contributions of KV heads to model accuracy. It also proposed a methodology to profile and quantify this contribution, which produces *head importance scores* in the range from 0 to 1, and heads with larger importance scores exhibit higher sensitivity to KV data. Inspired by this, we aim to leverage *head importance* to address the above-mentioned challenges.

Adaptive threshold configuration. Generally, we assign a larger threshold to the attention head with larger importance score to protect its effective information. First, we select an upper bound threshold η for all heads. Subsequently, for an attention head i with importance score s_i , its reuse threshold τ_i is computed by

$$\theta^* = \arccos(\eta) \quad (7)$$

$$\theta_i = \lambda_i \theta^* + (1 - \lambda_i) \pi \quad (8)$$

$$\tau_i = \cos(\theta_i) \quad (9)$$

Here, Equation (7) converts similarity threshold upper bound η into an angle threshold upper bound θ . In Equation (8), the coefficient $\lambda_i = s_i^p$, which determines the actual angle threshold θ_i for head i according to its importance. Equation (9) yields the final similarity threshold. In practice, one can set p to 2 or 3 in which case most attention heads have a high reuse rate while the truly important heads can be timely updated, ensuring both effectiveness and efficiency.

Intra-GQA aggregation. In order to apply our method to GQA scenarios, we need first define the importance of each query head. Though [46] only gave the method to compute the importance score of KV heads, we show that such a method can also be utilized to compute the importance score of query heads, with a slight modification. The detailed process is given in Appendix A. Now we can give our intra-GQA aggregation method based on the query head importance. To ensure accuracy, we adopt a conservative aggregation manner that follows the two rules:

- The query head with larger importance score should account for a higher proportion during the aggregation.
- The aggregation result should be mainly determined by the query heads with low cosine similarities, especially when they have large importance scores.

Considering a query group including m query heads, denoted by q_1, q_2, \dots, q_m , whose importance scores are s_1, s_2, \dots, s_m . Assume that at one step, the cosine similarities are $\text{sim}_1, \text{sim}_2, \dots, \text{sim}_m$, respectively, and then the aggregated similarity s is expressed by

$$s = \frac{s_1 + s_2 + \dots + s_m}{\frac{s_1}{\text{sim}_1} + \frac{s_2}{\text{sim}_2} + \dots + \frac{s_m}{\text{sim}_m}}. \quad (10)$$

Such an aggregation satisfies the above two rules. And in addition, when all the query heads have the same cosine similarities, the aggregation result maintains the same value, which is reasonable.

3.3 Handling Hard-to-Reuse Heads

The proposed cache policy may encounter some hard-to-reuse heads. For example, if a KV head exhibits high importance but low cosine similarity, according to Equation (7) - (9), it typically leads to a strict high reuse threshold and low cache hit rate. To address such heads, firstly, we try to use the *speculative sparse prefetching* technique described in Section 2.2 to enable the PCIe transfer of cache-missed KV heads to be overlapped by GPU computation. However, due to the low PCIe bandwidth, the transfer latency can only be partially overlapped. To further eliminate the transfer overhead, we propose *persist caching*, which retains the full KVCache of unprefetchable hard-to-reuse heads in GPU HBM. Before detailing this technique, we need to first quantify the *reuse difficulty* of the KV heads:

Quantifying reuse difficulty. We define the reuse difficulty of a KV head, denoted by D_i , as

$$D_i = \tau_i - (\hat{s}_i - \epsilon), \quad (11)$$

where τ_i is the similarity threshold of this KV head and \hat{s}_i is its offline profiled average cosine similarity, which is evaluated on adjacent query pairs generated by tens of random sequences. $\epsilon > 0$ is an error tolerance margin.

Persistent caching. We select heads with high D_i and retain their full KVCache in GPU HBM. This is feasible because the memory size of our cache data buffer equals the top- k KV data size (e.g., only 10% of the total KVCache), leaving substantial free capacity in GPU HBM. In practice, for each layer, we compute N_p , the number of prefetchable heads, by

$$N_p = \frac{T_{comp}}{B_{PCIe} * \text{mem}_{head}}, \quad (12)$$

where B_{PCIe} is the peak PCIe bandwidth, mem_{head} is the size of top- k KV data of a single head, and T_{comp} is the per-layer GPU computation latency. Given the maximum token number during decoding (configured by the user), we profile T_{comp} through a single system pre-run. Then, we calculate the number of HBM-persistent heads for each layer by

$$N_{persist}^l = \max(N_d^l - N_p, 0), \quad (13)$$

where N_d^l denotes the number of heads with $D_i > 0$ for layer l . Specially, following [16], we retain all the KV heads

of the first layer in HBM since they cannot be prefetched. In addition, if the HBM budget is insufficient, we prioritize the heads with the highest D_i to maximize the performance gains from persistent caching.

4 System Design

In this section, we present CLO, a CPU-light LLM inference system with KVCache offloading, top- k attention and dynamic GPU caching. CLO employs the head-wise light-weight cache described in Section 3 as its core component. Section 4.1 provides the system overview and Section 4.2 details its workflow. Additionally, CLO redesigns the CPU-to-GPU data transmission stack with (1) a zero-copy transfer engine bypassing CPU-side data gathering to improve PCIe bandwidth utilization (Section 4.3), and (2) a novel GPU-centric transmission synchronization mechanism ensuring uninterrupted kernel launch to reduce GPU idle time (Section 4.4).

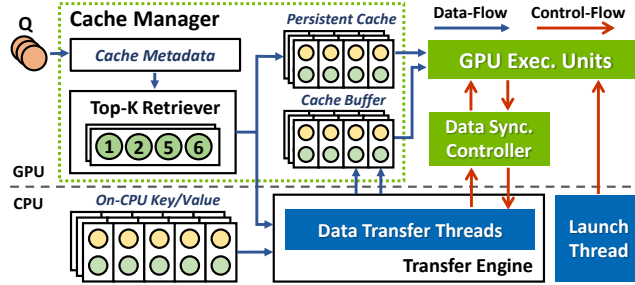


Figure 8. System overview of CLO.

4.1 Overview

Figure 8 provides an overview of CLO. It comprises the following core components:

Cache Manager. This module manages KVCache storage, loading and caching. As described in Section 3.3, at the head granularity, KVCache is partitioned into Persistent Cache and offloaded On-CPU Key/Value. Management of the former follows conventional full-GPU KVCache, whose details we omit here. The loading and GPU caching of On-CPU Key/Value are managed through speculative sparse prefetching (Section 2.2, *prefetching* in short) and query similarity-based approximate cache (Section 3.1, *similarity cache* in short). Cache Metadata records the KVCache partition results for dispatching KV loading requests. Also, it stores query labels, the metadata of similarity cache. The data buffer of similarity cache is referred to as Cache Buffer. In addition, Cache Manager employs a Top- k Retriever, with which CLO can perform fast top- k KV vector selection using a SOTA top- k algorithm HATA [9].

Transfer Engine. This component executes the CPU-to-GPU KV data transfer. It employs several dedicated CPU

Data Transfer Threads to send required top- k KV data to the Cache Buffer in GPU HBM via zero-copy operation.

Data Synchronization Controller. This module performs GPU-centric data transfer synchronization, which exclusively blocks GPU execution when needed. For kernel launching, CLO assigns it to a separate CPU Launch Thread. This design allows for uninterrupted kernel launching.

4.2 Inference Workflow

Initialization. During CLO’s initialization phase, KVCache heads are partitioned into HBM-persistent-cached ones and offloaded ones following the strategy detailed in Section 3.3. This partitioning leverages offline-profiled data, including head importance, average cosine similarity, and prefetchable head counts.

Prefill phase. CLO introduces two operations to the prefill phase. First, following the top- k attention algorithm it used, CLO encodes the KVCache into top- k retrieval metadata as presented in Section 2.2. This is typically low-overhead compared to other computations during prefill phase [9]. Second, CLO offloads partial or full KV heads to the host memory based on the initialization partitioning results. This process is asynchronously executed alongside the GPU computation tasks, with its overhead being fully overlapped.

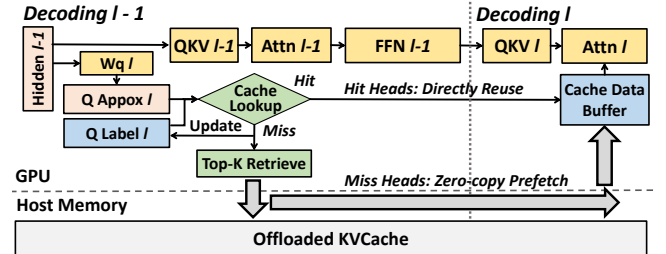


Figure 9. Inference workflow of CLO during the decoding phase. For clarity, only processes relevant to cache accessing and host data prefetching for layer l are depicted.

Decoding phase. During decoding, CLO dynamically retrieves and loads the top- k KV data for each step. Figure 9 illustrates the workflow of CLO’s decoding phase. For layer l , CLO begins to retrieve and load its top- k KV data at the beginning of layer $l - 1$. It computes an approximate query vector using Equation 5, which is employed to perform the cache lookup to identify hit heads. For missed heads, CLO retrieves new top- k KV data and launches their prefetching. Then, it continues to execute the remaining computation of layer $l - 1$ (attention, FFN). Note that the prefetching mechanism splits the cache update into two phases, namely *query labels update* and *KV data update*. Query labels for missed heads are immediately updated upon the finish of cache lookup, while their KV is gradually updated during the prefetching. After the qkv projection in layer l , CLO retrieves top- k KV data of HBM-persistent-cached heads using

layer l ’s actual query vector. Finally, after the prefetching completes, the GPU Execution Units begin to perform layer l ’s attention computation using data from both Cache Buffer and Persistent Cache, as shown in Figure 8.

4.3 Zero-Copy Transfer Engine

CLO employs a zero-copy engine for CPU-to-GPU data transfer, eliminating redundant KV data gathering on CPU, maximizing PCIe bandwidth, and reducing transfer latency.

Zero-copy is a key system optimization technology that directly transfers data from source to destination without extra data movement. To enable zero-copy in CPU-to-GPU data transfer, we build our transfer engine on GDRCopy [22], which leverages the PCIe BAR [1] area to expose the GPU memory to the CPU, enabling direct CPU access to GPU memory via LD/ST instructions.

Based on the GDRCopy, the zero-copy engine maintains a thread pool, with each thread transferring KV data at the granularity of a single K/V vector. Notably, the length of K/V vectors (128 FP16 elements) aligns well with the 64-byte transmission granularity of PCIe. To further accelerate the CPU-to-GPU zero-copy, the transfer engine leverages AVX SIMD instructions [13] to boost the data transfer efficiency, and utilizes CPU cache prefetching [2] to pre-load the subsequent KV data to mitigate the impact of random CPU memory access. With these optimizations, the zero-copy engine requires only 4 CPU threads to saturate PCIe 4.0 bandwidth, as demonstrated in Section 6.5.

4.4 GPU-Centric Data Synchronization

To eliminate the kernel launch overhead caused by CPU-centric synchronization, we design a GPU-centric transmission synchronization mechanism, which blocks the GPU execution instead of the CPU, which ensures that CPU threads can continuously launch GPU kernels.

We decouple kernel launching from data transmission and synchronization tasks by assigning them to a separate CPU thread. And the data synchronization is performed via identifier variables in CPU-GPU shared memory. This design prevents CPU-side kernel launching from being stalled by transfer synchronization. Specifically, when a transfer is requested, the GPU writes KV data indices to host memory through Unified Virtual Addressing (UVA) and sets the corresponding identifiers in shared memory to trigger the transfer engine. Upon completion of the transfer, the transfer engine updates these identifiers to notify the GPU. The GPU polls these identifiers and proceeds with subsequent kernels only after confirming that the data transfer has finished.

5 Implementation Details

CLO is implemented based on FlashInfer [48] and Transformers [43], with 3417 lines of CUDA/C++ code and 1555 lines of Python code. Beyond the aforementioned efficient

system design and optimizations, CLO has also integrated the following additional optimizations to further improve the inference performance:

Kernel fusion for cache lookup and query label update. As described in Section 4.2, in CLO’s workflow, query label update immediately follows the cache lookup. Both of them require to access the incoming query vector and the historical query labels. Consequently, we fuse their kernels into a single one to reduce HBM access overhead and alleviate the pressure of the CPU kernel launching.

Hybrid attention kernel. CLO’s top- k attention computation requires accessing data from the Cache Buffer and the Persistent Cache. To address this hybrid data layout, we implement an attention kernel based on FlashAttention2 [7], which directly accesses data from both buffers, without the need for a separate data gathering operation. This implementation effectively reduces the HBM access overhead.

6 Evaluation

6.1 Experimental Setup

Platform and Models. All evaluations were run on a single machine with an AMD EPYC 9654 96-core CPU, a GPU with 48 GB HBM and 149.7 TFLOPS peak FP16 throughput (connected via PCIe 4.0 x16). Two open-source FP16 LLMs were tested: Llama3-8B-Instruct-1048K [27] (32 layers, 32 Q heads and 8 KV heads per layer) and Qwen2.5-14B-Instruct-1M [32] (48 layers, 40 Q heads and 8 KV heads per layer).

Benchmarks. We evaluated CLO on two benchmarks. First, *RULER* [11], which includes 13 subtasks (e.g., retrieval, multi-hop tracking, aggregation, QA) with configurable context lengths. Second, *LongBench* [3], which covers diverse real-world tasks (e.g., summarization, QA, code comprehension) with varying text lengths.

Baselines and configurations. We compare CLO with SOTA KVCache offloading baselines, RetroInfer [5] and InfiniGen [16]. RetroInfer leverages an LRU GPU cache to reduce data transfer, while InfiniGen hides transfer overhead via prefetching. We also include the full-attention implementation (storing all KVCache on GPU) to highlight CLO’s advantages. For all the offloading baselines, sparsity is fixed at 10% of total KV pairs. For CLO, we integrate a SOTA top- k attention algorithm HATA [9] (hash bits=256) for evaluation. For the hyperparameters introduced by CLO, we set $\eta = 0.8$ in Equation 7 and $p = 3$ for $\lambda_i = s_i^p$ in Equation 8 for both models. The parameter ϵ in Equation 11 is set to 0.1 for Llama3-8B and 0.05 for Qwen2.5-14B. These hyperparameters are manually tuned, but only once per model, which incurs acceptable overhead.

6.2 Performance Analysis

We first present the performance of different methods in Figure 10. CLO achieves high performance in both prefill and

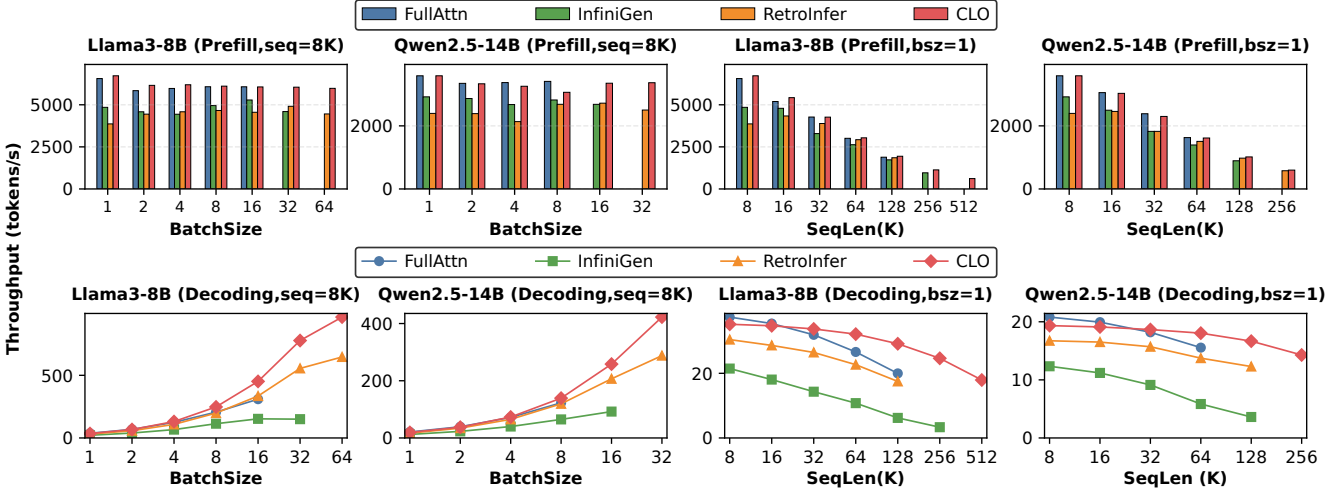


Figure 10. End-to-end prefill and decoding throughput across varying batch sizes and sequence lengths.

Table 3. GPU cache memory usage (GB) vs. total tokens

Methods	Llama3-8B, #tokens					Qwen2.5-14B, #tokens				
	32K	64K	128K	256K	512K	16K	32K	64K	128K	256K
RetroInfer	1.20	2.40	4.80	9.56	19.12	0.90	1.79	3.59	7.20	14.34
CLO	0.53	1.09	2.62	8.19	14.09	0.37	0.74	1.49	3.44	8.03

Table 4. Cache hit ratio (%)

Methods	Llama3-8B, SeqLen=8K					Qwen2.5-14B, SeqLen=8K				
	4	8	16	32	64	2	4	8	16	32
RetroInfer	90.41	90.15	90.08	90.07	90.05	92.65	91.33	91.42	91.34	91.35
CLO	79.54	74.69	76.69	84.99	80.00	80.62	80.65	80.65	81.53	80.75
Methods	Llama3-8B, Bsz=1					Qwen2.5-14B, Bsz=1				
	32K	64K	128K	256K	512K	16K	32K	64K	128K	256K
RetroInfer	91.21	91.41	91.44	-	-	93.11	93.08	93.43	93.07	-
CLO	83.48	82.60	84.05	90.11	88.57	75.78	73.88	65.20	72.52	68.27

decoding compared to other methods. Some results of baselines are missing due to GPU out-of-memory (OOM) errors or execution errors of their open-source implementations.

For prefill performance, across both models and various configurations, CLO closely matches FullAttn, while InfiniGen and RetroInfer lag behind. CLO leverages HATA, which incurs minimal retrieval metadata construction overhead for top- k attention. In contrast, RetroInfer suffers from cache and high retrieval metadata construction overhead, and InfiniGen is slowed by inefficient prefill implementation.

For decoding, CLO also demonstrates superior decoding performance across all configurations. It delivers a speedup of 1.16–1.67 \times on Llama3 and 1.09–1.47 \times on Qwen2.5 compared to the leading baseline.

The throughput of CLO scales significantly with increasing batch size, consistently outperforming other methods on both models. For short sequences, FullAttn is the top performer because attention is not the primary bottleneck, and other systems incur overhead from top- k retrieval. However, as the sequence length grows, CLO maintains higher throughput. InfiniGen shows the lowest performance, hindered by significant, unhidden data transfer overheads. Similarly, RetroInfer is slowed by increased cache management overheads as task size grows.

GPU cache memory usage and cache hit ratio. Both CLO and RetroInfer utilize on-GPU cache to reduce PCIe data transfers. Table 3 shows GPU cache memory usage, while Table 4 reports the cache hit ratios corresponding to the experiments in Figure 10. CLO uses significantly less GPU cache, consuming only an average of 47.6% of the memory required by RetroInfer. While RetroInfer achieves a higher cache hit ratio, its heavy LRU management constrains overall performance. By leveraging the query similarity-based approximate cache strategy, CLO achieves an average cache hit ratio of 79.22% while boosting throughput through lightweight cache management and speculative sparse prefetching for the transfer of missing data.

6.3 Accuracy Evaluation

Table 5 reports the average inference accuracy of different methods on LongBench and RULER. CLO consistently preserves accuracy with the HATA top- k attention algorithm, achieving results close to the original models with a maximum average drop of only 0.42. Also, it matches or outperforms the original HATA method. And on RULER, accuracy remains stable even as the sequence length grows, demonstrating robustness in long-context tasks. For both Qwen2.5-14B and Llama3-8B, CLO matches the best baselines, avoiding the drops seen in InfiniGen. These results

Table 5. Inference accuracy results.

Methods	LongBench	RULER			
		16K	32K	64K	128K
Qwen2.5-14B	53.34	94.35	94.48	92.29	88.85
RetroInfer	54.71	94.73	94.41	92.37	89.49
InfiniGen	52.74	92.78	92.19	89.74	85.26
HATA	53.19	94.06	94.13	92.24	88.47
CLO + HATA	53.15	94.36	94.22	92.35	88.94
Llama3-8B	41.06	86.07	80.80	76.26	72.96
RetroInfer	41.11	86.36	80.64	76.26	72.73
InfiniGen	40.22	79.70	76.76	72.96	69.37
HATA	41.58	86.56	80.94	76.28	73.87
CLO + HATA	41.15	85.65	80.70	75.94	73.44

demonstrate that CLO shows efficient offloading without sacrificing inference quality.

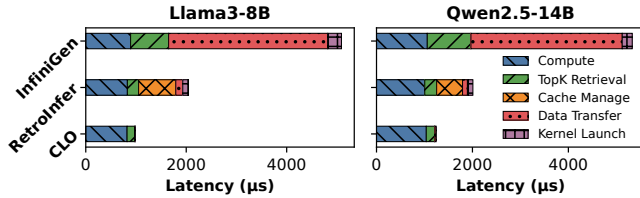


Figure 11. Per-layer decoding latency breakdown, evaluated with batch size=1 and sequence length=128K.

6.4 Breakdown Analysis

We further analyze the per-layer decoding latency of CLO, InfiniGen, and RetroInfer, as shown in Figure 11. CLO achieves a 2.1–5.2× speedup on Llama3 and 1.6–4.2× on Qwen2.5 compared to RetroInfer and InfiniGen, demonstrating its efficiency.

Cache management overhead in CLO is minimal due to its lightweight caching strategy, whereas RetroInfer spends 26.9–36.2% of decoding time on cache management, and InfiniGen has no cache management by design. The data transfer overhead is low for both RetroInfer and CLO. RetroInfer benefits from a high cache hit ratio, whereas CLO leverages speculative sparse prefetching to overlap the transfer of small-volume unhit data with computation. InfiniGen also uses speculative prefetching, but the large CPU-to-GPU data volume and inefficient PCIe transfer hinder full overlap.

Kernel launch overhead in CLO is negligible thanks to the GPU-centric Transfer Synchronization, which blocks GPU execution rather than CPU kernel launching. In contrast, InfiniGen and RetroInfer exhibit kernel launch overheads of up to 273.2 μs and 114.5 μs, respectively. Moreover, CLO also achieves lower top- k retrieval costs by leveraging the more efficient HATA attention algorithm, outperforming the top- k algorithms in InfiniGen and RetroInfer.

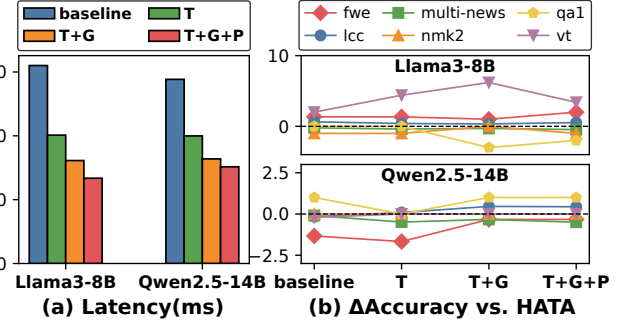


Figure 12. Ablation study of CLO’s cache strategy optimizations. **(a) End-to-end decoding step latency.** Llama3-8B is evaluated with batch size=64 and sequence length=8K. Qwen2.5-14B is evaluated with batch size=32 and sequence length=8K. **(b) Accuracy.** Evaluated on LongBench (lcc, multi-news) and RULER-128K (nmk2, fwe, qa1, vt).

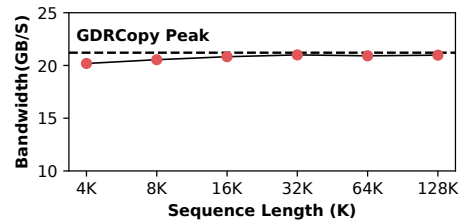


Figure 13. The PCIe bandwidth achieved during the data transfer process in CLO when using 4 CPU threads.

6.5 Effects of Optimizations

Optimizations for cache strategy. Figure 12 presents an ablation study of the optimizations presented in Section 3.2 and 3.3: **T** (adaptive Threshold configuration), **G** (intra-QA aggregation) and **P** (Persistent caching). Additionally, **baseline** applies a fixed threshold, and uses the minimum cosine similarities within query groups for cache lookup. All of them enable the speculative sparse prefetching. In Figure 12 (a), **baseline** yields high decoding latency on both Llama3 and Qwen2.5. Compared with **baseline**, for **T**, latency is reduced by 35.2% and 30.7%, followed by additional reductions of 48.0% and 43.2% with **G**. Applying **P** further decreases latency by 56.9% and 47.5%. These results demonstrate the effectiveness of each optimization.

Although these optimizations may impact inference accuracy, our proper settings for hyperparameters (see Section 6.1) maintain performance close to the original HATA across most datasets, as shown in Figure 12 (b), where HATA serves as the baseline and positive/negative values denote improvements/degradations. Furthermore, as elaborated in Section 6.3, the final average inference quality remains on par with both HATA and FullAttn. Considering the significant performance improvements achieved, this trade-off is deemed acceptable.

Transfer engine efficiency. Figure 13 shows the PCIe bandwidth achieved by CLO using 4 CPU threads, demonstrating the efficiency of its zero-copy transfer engine. As the sequence length increases from 4K to 128K, the bandwidth remains stable, approaching the GDRCopy peak of 21.21 GB/s. This indicates that the transfer engine delivers high, consistent PCIe bandwidth with low CPU overhead.

7 Related Works

The KVCache is a major memory bottleneck in LLM inference, there are two main categories of approaches that attempt to address this problem:

KVCache offloading is a class of approaches aimed at enhancing the system’s *scale-up* capability. Systems adopting this approach offload the KVCache to CPU memory to relieve GPU memory pressure, but focus on different optimization directions. Systems like InfLLM [45], MagicPiG [6] and ShadowKV [39] focus on improving top-*k* attention algorithms rather than addressing system-level challenges. PQCache [50] and RetroInfer [5] mitigate PCIe transfer volumes through GPU caching, yet they fail to account for the cache management overhead incurred by the CPU. Prefetching approaches, including FlexGen [36] and InfiniGen [16], help alleviate PCIe data transfer latency but face limitations in handling large-scale tasks or entail performance trade-offs. Overall, these methods tend to overlook CPU-side burdens and complexity of implementation.

Distributed KVCache partitions a model’s KVCache across multiple GPUs, thereby providing the system with *scale-out* capability. Tensor parallelism [28, 37, 52] partitions KVCache by attention heads, pipeline parallelism [12, 21, 29, 37] by layers, and sequence parallelism [17, 18, 44] by tokens, with each GPU storing only its shard. All these methods trade distributed communication for reduced GPU memory usage and are orthogonal to scale-up approaches such as CLO.

8 Conclusion

We present CLO, a CPU-light LLM inference system with KV-Cache offloading, top-*k* attention, and dynamic GPU caching. CLO optimizes decoding performance through light-weight caching strategy, computation-transfer overlap, and optimized data-transfer stack. Through these optimizations, CLO eliminates the CPU bottlenecks in existing systems and fully utilizes the hardware resources like GPU HBM and PCIe bandwidth. We provide a high performance implementation for CLO, which improves inference throughput by 9.3%–66.6% compared to SOTA baseline while preserving inference accuracy.

References

- [1] AMD. 2023. PCIe Base Address Registers. <https://docs.amd.com/r/en-US/pg055-axi-bridge-pcie/PCIe-Base-Address-Registers>. accessed, Aug. 2025.
- [2] ArmDeveloper. 2025. Cache prefetching. <https://learn.arm.com/learning-paths/cross-platform/memory-latency/latency-and-cache-prefetching/>. accessed, Aug. 2025.
- [3] Yushi Bai, Xin Lv, Jiajie Zhang, Hongchang Lyu, Jiankai Tang, Zhiidian Huang, Zhengxiao Du, Xiao Liu, Aohan Zeng, Lei Hou, Yuxiao Dong, Jie Tang, and Juanzi Li. 2024. LongBench: A Bilingual, Multitask Benchmark for Long Context Understanding. In *Proceedings of the 62nd Annual Meeting of the Association for Computational Linguistics (Volume 1: Long Papers)*, Lun-Wei Ku, Andre Martins, and Vivek Srikumar (Eds.). Association for Computational Linguistics, Bangkok, Thailand, 3119–3137. doi:10.18653/v1/2024.acl-long.172
- [4] Ramakrishna Bairi, Atharv Sonwane, Aditya Kanade, Vageesh D C, Arun Iyer, Suresh Parthasarathy, Sriram Rajamani, Balasubramanyan Ashok, and Shashank Shet. 2024. Codeplan: Repository-level coding using llms and planning. *Proceedings of the ACM on Software Engineering* 1, FSE (2024), 675–698.
- [5] Yaoqi Chen, Jinkai Zhang, Baotong Lu, Qianxi Zhang, Chengruidong Zhang, Jingjia Luo, Di Liu, Huiqiang Jiang, Qi Chen, Jing Liu, et al. 2025. RetroInfer: A Vector-Storage Approach for Scalable Long-Context LLM Inference. *arXiv preprint arXiv:2505.02922* (2025).
- [6] Zhuoming Chen, Ranajoy Sadhukhan, Zihao Ye, Yang Zhou, Jianyu Zhang, Niklas Nolte, Yuandong Tian, Matthijs Douze, Leon Bottou, Zhihao Jia, and Beidi Chen. 2025. MagicPIG: LSH Sampling for Efficient LLM Generation. In *The Thirteenth International Conference on Learning Representations*. <https://openreview.net/forum?id=ALzTQUGw8a>
- [7] Tri Dao. 2024. FlashAttention-2: Faster Attention with Better Parallelism and Work Partitioning. In *The Twelfth International Conference on Learning Representations*. <https://openreview.net/forum?id=mZn2Xyh9Ec>
- [8] Bin Gao, Zhuomin He, Puru Sharma, Qingxuan Kang, Djordje Jevdjic, Junbo Deng, Xingkun Yang, Zhou Yu, and Pengfei Zuo. 2024. Cost-Efficient large language model serving for multi-turn conversations with CachedAttention. In *2024 USENIX Annual Technical Conference (USENIX ATC 24)*. 111–126.
- [9] Ping Gong, Jiawei Yi, Shengnan Wang, Juncheng Zhang, Zewen Jin, Ouxiang Zhou, Ruibo Liu, Guanbin Xu, Youhui Bai, Bowen Ye, Kun Yuan, Tong Yang, Gong Zhang, Renhai Chen, Feng Wu, and Cheng Li. 2025. HATA: Trainable and Hardware-Efficient Hash-Aware Top-*k* Attention for Scalable Large Model Inference. In *Findings of the Association for Computational Linguistics: ACL 2025*, Wanxiang Che, Joyce Nabende, Ekaterina Shutova, and Mohammad Taher Pilehvar (Eds.). Association for Computational Linguistics, Vienna, Austria, 24856–24871. <https://aclanthology.org/2025.findings-acl.1275/>
- [10] Ankit Gupta, Guy Dar, Shaya Goodman, David Ciprut, and Jonathan Berant. 2021. Memory-efficient Transformers via Top-*k* Attention. In *Proceedings of the Second Workshop on Simple and Efficient Natural Language Processing*, Nafise Sadat Moosavi, Iryna Gurevych, Angela Fan, Thomas Wolf, Yufang Hou, Ana Marasović, and Sujith Ravi (Eds.). Association for Computational Linguistics, Virtual, 39–52. doi:10.18653/v1/2021.sustainlp-1.5
- [11] Cheng-Ping Hsieh, Simeng Sun, Samuel Kriman, Shantanu Acharya, Dima Rekesh, Fei Jia, and Boris Ginsburg. 2024. RULER: What’s the Real Context Size of Your Long-Context Language Models?. In *First Conference on Language Modeling*. <https://openreview.net/forum?id=kloBbc76Sy>
- [12] Yanping Huang, Youlong Cheng, Ankur Bapna, Orhan Firat, Mia Xu Chen, Dehao Chen, HyoukJoong Lee, Jiquan Ngiam, Quoc V. Le, Yonghui Wu, and Zhifeng Chen. 2019. *GPipe: efficient training of giant neural networks using pipeline parallelism*. Curran Associates Inc., Red Hook, NY, USA.
- [13] Intel. 2017. AVX-512 Instructions. <https://www.intel.com/content/www/us/en/developer/articles/technical/intel-avx-512-instructions.html>. accessed, Aug. 2025.

[14] Juyong Jiang, Fan Wang, Jiasi Shen, Sungju Kim, and Sunghun Kim. 2024. A survey on large language models for code generation. *arXiv preprint arXiv:2406.00515* (2024).

[15] Huan Yee Koh, Jiaxin Ju, Ming Liu, and Shirui Pan. 2022. An empirical survey on long document summarization: Datasets, models, and metrics. *ACM computing surveys* 55, 8 (2022), 1–35.

[16] Wonbeom Lee, Jungi Lee, Junghwan Seo, and Jaewoong Sim. 2024. InfiniGen: Efficient generative inference of large language models with dynamic KV cache management. In *18th USENIX Symposium on Operating Systems Design and Implementation (OSDI 24)*. 155–172.

[17] Shenggui Li, Fuzhao Xue, Chaitanya Baranwal, Yongbin Li, and Yang You. 2023. Sequence Parallelism: Long Sequence Training from System Perspective. In *Proceedings of the 61st Annual Meeting of the Association for Computational Linguistics (Volume 1: Long Papers)*, Anna Rogers, Jordan Boyd-Graber, and Naoki Okazaki (Eds.). Association for Computational Linguistics, Toronto, Canada, 2391–2404. doi:10.18653/v1/2023.acl-long.134

[18] Hao Liu, Matei Zaharia, and Pieter Abbeel. 2024. RingAttention with Blockwise Transformers for Near-Infinite Context. In *The Twelfth International Conference on Learning Representations*. <https://openreview.net/forum?id=WsRHpHH4s0>

[19] Nimrod Megiddo and Dharmendra S Modha. 2003. ARC: A Self-Tuning, low overhead replacement cache. In *2nd USENIX Conference on File and Storage Technologies (FAST 03)*.

[20] MetaAI. 2024. Introducing Llama 3.1: Our most capable models to date. <https://ai.meta.com/blog/meta-llama-3-1/>. accessed, Aug. 2025.

[21] Deepak Narayanan, Mohammad Shoeybi, Jared Casper, Patrick LeGresley, Mostofa Patwary, Vijay Korthikanti, Dmitri Vainbrand, Prethvi Kashinkunti, Julie Bernauer, Bryan Catanzaro, Amar Phanishayee, and Matei Zaharia. 2021. Efficient large-scale language model training on GPU clusters using megatron-LM. In *Proceedings of the International Conference for High Performance Computing, Networking, Storage and Analysis* (St. Louis, Missouri) (SC ’21). Association for Computing Machinery, New York, NY, USA, Article 58, 15 pages. doi:10.1145/3458817.3476209

[22] NVIDIA. 2021. Magnum IO GDRCopy: Enable faster memory transfers between CPU and GPU with GDRCopy. <https://developer.nvidia.com/gdrcopy>. accessed, Aug. 2025.

[23] NVIDIA. 2025. NVIDIA A100 Tensor Core GPU. <https://www.nvidia.com/content/dam/en-xx/Solutions/Data-Center/a100/pdf/nvidia-a100-datasheet-us-nvidia-1758950-r4-web.pdf>. accessed, Aug. 2025.

[24] NVIDIA. 2025. NVIDIA A40 datasheet. <https://images.nvidia.com/content/Solutions/data-center/a40/nvidia-a40-datasheet.pdf>. accessed, Aug. 2025.

[25] NVIDIA. 2025. NVIDIA H100 datasheet. <https://resources.nvidia.com/en-us-gpu-resources/h100-datasheet-24306>. accessed, Aug. 2025.

[26] Elizabeth J O’neil, Patrick E O’neil, and Gerhard Weikum. 1993. The LRU-K page replacement algorithm for database disk buffering. *AcM Sigmod Record* 22, 2 (1993), 297–306.

[27] Leonid Pekelis, Michael Feil, Forrest Moret, Mark Huang, and Tiffany Peng. 2024. Llama 3 Gradient: A series of long context models. doi:10.57967/hf/3372

[28] PyTorch. 2024. Large Scale Transformer model training with Tensor Parallel. https://docs.pytorch.org/tutorials/intermediate/TP_tutorial.html. accessed, Aug. 2025.

[29] PyTorch. 2025. Pipeline Parallelism. <https://docs.pytorch.org/docs/stable/distributed.pipeline.html>. accessed, Aug. 2025.

[30] Libo Qin, Qiguang Chen, Xiachong Feng, Yang Wu, Yongheng Zhang, Yinghui Li, Min Li, Wanxiang Che, and Philip S Yu. 2024. Large language models meet nlp: A survey. *arXiv preprint arXiv:2405.12819* (2024).

[31] Ziyue Qiu, Juncheng Yang, Juncheng Zhang, Cheng Li, Xiaosong Ma, Qi Chen, Mao Yang, and Yinlong Xu. 2023. FrozenHot Cache: Rethinking Cache Management for Modern Hardware. In *Proceedings of the Eighteenth European Conference on Computer Systems (Rome, Italy) (EuroSys ’23)*. Association for Computing Machinery, New York, NY, USA, 557–573. doi:10.1145/3552326.3587446

[32] QwenTeam. 2025. Qwen2.5-1M: Deploy Your Own Qwen with Context Length up to 1M Tokens. <https://qwenlm.github.io/blog/qwen2.5-1m/>. accessed, Aug. 2025.

[33] Luka Ribar, Ivan Chelombiev, Luke Hudlass-Galley, Charlie Blake, Carlo Luschi, and Douglas Orr. 2024. SparQ attention: bandwidth-efficient LLM inference. In *Proceedings of the 41st International Conference on Machine Learning* (Vienna, Austria) (ICML ’24). JMLR.org, Article 1731, 26 pages.

[34] John T Robinson and Murthy V Devarakonda. 1990. Data cache management using frequency-based replacement. In *Proceedings of the 1990 ACM SIGMETRICS conference on Measurement and modeling of computer systems*. 134–142.

[35] Jiacheng Shen, Pengfei Zuo, Xuchuan Luo, Yuxin Su, Jiazheng Gu, Hao Feng, Yangfan Zhou, and Michael R. Lyu. 2023. Ditto: An Elastic and Adaptive Memory-Disaggregated Caching System. In *Proceedings of the 29th Symposium on Operating Systems Principles* (Koblenz, Germany) (SOSP ’23). Association for Computing Machinery, New York, NY, USA, 675–691. doi:10.1145/3600006.3613144

[36] Ying Sheng, Lianmin Zheng, Binhang Yuan, Zhuohan Li, Max Ryabinin, Beidi Chen, Percy Liang, Christopher Ré, Ion Stoica, and Ce Zhang. 2023. Flexgen: High-throughput generative inference of large language models with a single gpu. In *International Conference on Machine Learning*. PMLR, 31094–31116.

[37] Mohammad Shoeybi, Mostofa Patwary, Raul Puri, Patrick LeGresley, Jared Casper, and Bryan Catanzaro. 2019. Megatron-LM: Training Multi-Billion Parameter Language Models Using Model Parallelism. *arXiv preprint arXiv:1909.08053* (2019).

[38] Prajwal Singhania, Siddharth Singh, Shwai He, Soheil Feizi, and Abhinav Bhatele. 2024. Loki: Low-rank keys for efficient sparse attention. *Advances in Neural Information Processing Systems* 37 (2024), 16692–16723.

[39] Hanshi Sun, Li-Wen Chang, Wenlei Bao, Size Zheng, Ningxin Zheng, Xin Liu, Harry Dong, Yuejie Chi, and Beidi Chen. 2024. ShadowKV: KV Cache in Shadows for High-Throughput Long-Context LLM Inference. *arXiv preprint arXiv:2410.21465* (2024).

[40] Jiaming Tang, Yilong Zhao, Kan Zhu, Guangxuan Xiao, Baris Kasikci, and Song Han. 2024. QUEST: query-aware sparsity for efficient long-context LLM inference. In *Proceedings of the 41st International Conference on Machine Learning* (Vienna, Austria) (ICML ’24). JMLR.org, Article 1955, 11 pages.

[41] Ashish Vaswani, Noam Shazeer, Niki Parmar, Jakob Uszkoreit, Llion Jones, Aidan N Gomez, Łukasz Kaiser, and Illia Polosukhin. 2017. Attention is all you need. *Advances in neural information processing systems* 30 (2017).

[42] Giuseppe Vietri, Liana V Rodriguez, Wendy A Martinez, Steven Lyons, Jason Liu, Raju Rangaswami, Ming Zhao, and Giri Narasimhan. 2018. Driving cache replacement with ML-based LeCaR. In *10th USENIX Workshop on Hot Topics in Storage and File Systems (HotStorage 18)*.

[43] Thomas Wolf, Lysandre Debut, Victor Sanh, Julien Chaumond, Clement Delangue, Anthony Moi, Pierrick Cistac, Tim Rault, Rémi Louf, Morgan Funtowicz, Joe Davison, Sam Shleifer, Patrick von Platen, Clara Ma, Yacine Jernite, Julien Plu, Canwen Xu, Teven Le Scao, Sylvain Gugger, Mariama Drame, Quentin Lhoest, and Alexander M. Rush. 2020. Transformers: State-of-the-Art Natural Language Processing. In *Proceedings of the 2020 Conference on Empirical Methods in Natural Language Processing: System Demonstrations*. Association for Computational Linguistics, Online, 38–45. <https://www.aclweb.org/anthology/2020.emnlp-demos.6>

[44] Bingyang Wu, Shengyu Liu, Yinmin Zhong, Peng Sun, Xuanzhe Liu, and Xin Jin. 2024. LoongServe: Efficiently Serving Long-Context Large Language Models with Elastic Sequence Parallelism. In *Proceedings*

of the ACM SIGOPS 30th Symposium on Operating Systems Principles (Austin, TX, USA) (SOSP '24). Association for Computing Machinery, New York, NY, USA, 640–654. doi:10.1145/3694715.3695948

[45] Chaojun Xiao, Penglle Zhang, Xu Han, Guangxuan Xiao, Yankai Lin, Zhengyan Zhang, Zhiyuan Liu, and Maosong Sun. 2024. Inflm: Training-free long-context extrapolation for llms with an efficient context memory. *Advances in Neural Information Processing Systems* 37 (2024), 119638–119661.

[46] Guangxuan Xiao, Jiaming Tang, Jingwei Zuo, junxian guo, Shang Yang, Haotian Tang, Yao Fu, and Song Han. 2025. DuoAttention: Efficient Long-Context LLM Inference with Retrieval and Streaming Heads. In *The Thirteenth International Conference on Learning Representations*. <https://openreview.net/forum?id=cFu7ze7xUm>

[47] Guangxuan Xiao, Yuandong Tian, Beidi Chen, Song Han, and Mike Lewis. 2024. Efficient Streaming Language Models with Attention Sinks. In *The Twelfth International Conference on Learning Representations*. <https://openreview.net/forum?id=NG7sS51zVF>

[48] Zihao Ye, Lequn Chen, Ruihang Lai, Wuwei Lin, Yineng Zhang, Stephanie Wang, Tianqi Chen, Baris Kasikci, Vinod Grover, Arvind Krishnamurthy, and Luis Ceze. 2025. FlashInfer: Efficient and Customizable Attention Engine for LLM Inference Serving. *arXiv preprint arXiv:2501.01005* (2025). <https://arxiv.org/abs/2501.01005>

[49] Shukang Yin, Chaoyou Fu, Sirui Zhao, Ke Li, Xing Sun, Tong Xu, and Enhong Chen. 2024. A survey on multimodal large language models. *National Science Review* 11, 12 (2024), nwae403.

[50] Hailin Zhang, Xiaodong Ji, Yilin Chen, Fangcheng Fu, Xupeng Miao, Xiaonan Nie, Weipeng Chen, and Bin Cui. 2025. Pqcache: Product quantization-based kvcache for long context llm inference. *Proceedings of the ACM on Management of Data* 3, 3 (2025), 1–30.

[51] Zhenyu Zhang, Ying Sheng, Tianyi Zhou, Tianlong Chen, Lianmin Zheng, Ruisi Cai, Zhao Song, Yuandong Tian, Christopher Ré, Clark Barrett, Zhangyang Wang, and Beidi Chen. 2023. H2O: heavy-hitter oracle for efficient generative inference of large language models. In *Proceedings of the 37th International Conference on Neural Information Processing Systems* (New Orleans, LA, USA) (NIPS '23). Curran Associates Inc., Red Hook, NY, USA, Article 1506, 50 pages.

[52] Lianmin Zheng, Liangsheng Yin, Zhiqiang Xie, Chuyue Sun, Jeff Huang, Cody Hao Yu, Shiyi Cao, Christos Kozyrakis, Ion Stoica, Joseph E. Gonzalez, Clark Barrett, and Ying Sheng. 2025. SGLang: efficient execution of structured language model programs. In *Proceedings of the 38th International Conference on Neural Information Processing Systems* (Vancouver, BC, Canada) (NIPS '24). Curran Associates Inc., Red Hook, NY, USA, Article 2000, 27 pages.

A Appendix: Query head importance

We first briefly review the method of obtaining the importance of kv heads, given by Duo-attention [46]. For each KV head j at layer i , its importance score is defined as $\alpha_{i,j} \in [0,1]$. The specific importance scores of the KV heads are determined by a lightweight training on a synthetic dataset with a self-defined loss function. During training, the attention output of each head j at layer i is expressed by

$$\text{attn}_{i,j} = \alpha_{i,j} * \text{full_attn}_{i,j} + (1 - \alpha_{i,j}) * \text{stream_attn}_{i,j} \quad (14)$$

where $\text{full_attn}_{i,j}$ represents the vanilla attention utilizing all the whole KV vectors and $\text{stream_attn}_{i,j}$ is a fast attention method proposed by [47], which only uses the sink tokens and recent tokens. According to [46], after training, the value of $\text{attn}_{i,j}$ can reflect the importance of the KV head j at layer i . In the multi-head attention (MHA) case, each KV head corresponds to a single query head, so $\text{attn}_{i,j}$ also represents the importance of the corresponding query head. While in the group-query attention (GQA) case, each KV head is shared by several query heads in a query group. To measure the importance of each query head in this situation, we rewrite Equation (14) as follows

$$\text{attn}_{i,j,l} = \alpha_{i,j,l} * \text{full_attn}_{i,j,l} + (1 - \alpha_{i,j,l}) * \text{stream_attn}_{i,j,l} \quad (15)$$

where $\text{attn}_{i,j,l}$ is the attention output of the l -th query head of group j at layer i . In Equation (14), $\text{full_attn}_{i,j}$, $\text{stream_attn}_{i,j}$ and $\text{attn}_{i,j}$ are the corresponding attention outputs of the query heads belonging group j , and all of these query heads

share a common importance score $\alpha_{i,j}$, while in Equation 15, each query head involves an individual importance score $\alpha_{i,j,l}$. For other details about importance score learning including training loss, datasets, as well as other related settings, please refer to [46].

In Figure 14, we visualize the head importance results obtained through the above training method.

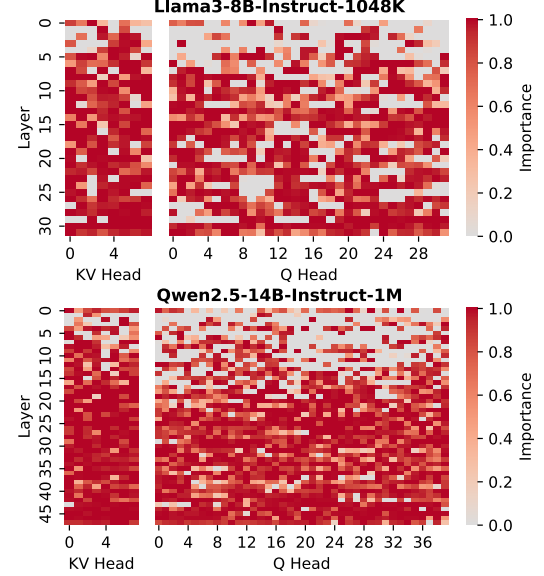


Figure 14. Query and KV head importance of Llama3-8B-Instruct-1048K [27] and Qwen2.5-14B-Instruct-1M [32].